2162-8769/2019/8(3)/R51/7/$38.00 © The Electrochemical Society

Selective Scattering of Blue and Red Light Based on Silver and Gold Nanocubes

Yiyang Ye[z] **and T. P. Chen**[z]

School of Electrical and Electronic Engineering, Nanyang Technological University, Singapore 639798, Singapore

Selective scattering of red, green, and blue light and transmitting other visible light to achieve a transparent projection screen has been proposed based on metallic nanoparticle's localized surface plasmon resonance (LSPR). However, of the many proposed structures, dielectric (TiO_2) substrate/silver (Ag) nanocube structure was only demonstrated to selectively scatter blue light in the backward direction. Therefore, for this setup, on one hand, it is of interest to enhance selective backward scattering of red light, and on the other hand, it is of interest to investigate ways of selective forward scattering of both blue and red light. Selective backward scattering may be used in applications such as heads up display (HUD), while selective forward scattering may be applied to, for example, display advertisements on shop windows. In this work, through numerical simulation, forward and backward scattering properties of dielectric substrate/Ag (or gold) nanocube structures were investigated. Based on these properties, three designs are proposed which can achieve selective scattering of blue and red light in forward or backward or both directions.
 [DOI: 10.1149/2.0131903jss]

Manuscript submitted February 7, 2019; revised manuscript received March 13, 2019. Published April 2, 2019.

Recently, the idea of wavelength-selective scattering of light to achieve a transparent projection screen has been proposed based on metallic nanoparticle's localized surface plasmon resonance (LSPR).[1–4] In the ideal case, metallic nanoparticles dispersed in a transparent matrix only selectively scatter red, green, and blue light and transmit visible light of other colors. Nanospheres and ellipsoids achieve selective scattering of red, green, or blue light by taking advantage of the nanoparticle's dipolar resonance peak,[1,3,4] while Ag nanocubes simultaneously achieve selective scattering of blue and red light by a splitting of resonance peak when it is placed on a dielectric substrate.[2] For the transparent projection screen achieved by depositing Ag nanocubes on TiO_2 thin film reported in previous work,[2] it only considers enhancement of backward scattering and its backward scattering of red light is much weaker than that of blue light. So, based of this, it is of interest to further enhance the backward scattering of red light. The resonance peak wavelength of the spectrum of selective backward scattering of blue light (around 460 nm) is quite close to the wavelength of green light (around 530 nm), and the spectrum of the selective backward scattering of blue light has not decreased to zero around the wavelength of green light,[2] which means even when no structure for selective backward scattering of green light is designed, backward scattering of green light still exists (but not as strong as that of blue light). In addition to this, human eyes are sensitive to green light.[5] So for the above two reasons, wo do not intend to enhance backward scattering of green light. Selective backward scattering is useful, because it can be applied to, for example, heads up display (HUD), where navigation or other information is shown on the windshield of a vehicle or of an aircraft. But some applications find selective forward scattering useful, one example is shop window advertisement where vivid images or movies are displayed on a window wall. For this reason, it is also of interest to determine how to achieve selective forward scattering of blue and red light. The reason why it is not desired to enhance forward scattering of green light is similar to that for the backward scattering as discussed above. In this work, scattering properties of Ag and gold (Au) nanocubes deposited on dielectric (TiO_2 or glass) substrate are studied, and three designs for selective scattering of blue and red light are shown, of which, only one is suitable for simultaneous forward and backward selective scattering of blue and red light, the other two are only suitable for either forward or backward selective scattering of blue and red light.

Simulation Methods

All simulated results shown in this work were calculated by a numerical simulation method known as Finite-Difference Time-Domain (FDTD).[6] The commercial software to implement FDTD is "FDTD Solutions". Because the refractive index of TiO_2 is controversial (values between 1.9 to 2.51 have been reported),[7,8] we experimentally measured its value. To determine the refractive index of TiO_2 to be used in the simulation, we deposited a layer of TiO_2 thin film with a thickness of 120 nm on a piece of silicon wafer by RF sputtering process followed by calcination at 500°C for 1 h. The refractive index averaged in the visible wavelength range (400–800 nm) of the TiO_2 thin film is 2.3 as obtained with spectroscopic ellipsometry.[9] For glass used in subsequent simulations, its refractive index is assumed to be 1.5. In subsequent simulations, for a metallic nanocube placed on dielectric substrate, back-scattered light is detected by a box-shaped monitor placed on the same side (with respect to the metallic nanocube) where light is injected (assuming incident light is perpendicular to the air/dielectric interface), whose face nearest and parallel to the air/dielectric interface is open and passes through the geometrical center of the metallic nanocube, while forward scattered light is collected by another box-shaped monitor placed on the other side, whose open-face shares the same plane with that of the back-scattered light monitor. In our simulation, the shared open-face of the two box-shaped monitors has a dimension of 400 by 400 nm. The source type is "Total-field scattered-field" (TFSF) so that only the scattered light will be detected by monitors.[10] The grid size of the three-dimensional mesh override region is 1 nm. The edge and corner of a metallic nanocube is rounded by a radius which is 10% of the metallic nanocube's edge length. The dielectric constants of Ag and Au are taken from reference.[11] The fitting of dielectric constants of Ag and Au to experimental data from reference is conducted by the commercial software "FDTD solutions". The fitted dielectric constants of Ag and Au satisfy Kramers-Kronig relation,[12] and have minimized error with respect to the experimental data from reference.

Results and Discussion

The resonance peak splitting of a Ag nanocube when it is placed on a dielectric substrate originates from the substrate-mediated coupling between a bright dipolar and a dark quadrupolar plasmon mode, and the higher the refractive index of the substrate, the larger the peak splitting.[13–18]

From our simulation, it is found that the scattering spectrum of a Ag nanocube is affected not only by the presence of dielectric substrate, but also by propagation direction of incident light when the Ag nanocube is placed on a dielectric substrate, as shown in Fig. 1, where the scattering cross section is the ratio of the total scattered power to power flux of the incident light. In Fig. 1, a splitting of scattering peak is observed when the Ag nanocube in air is placed on TiO_2 substrate, and the scattering peak around 440 nm is stronger than that around 710 nm when light is incident from air to TiO_2 substrate

[z]E-mail: yeyi0005@e.ntu.edu.sg; echentp@ntu.edu.sg

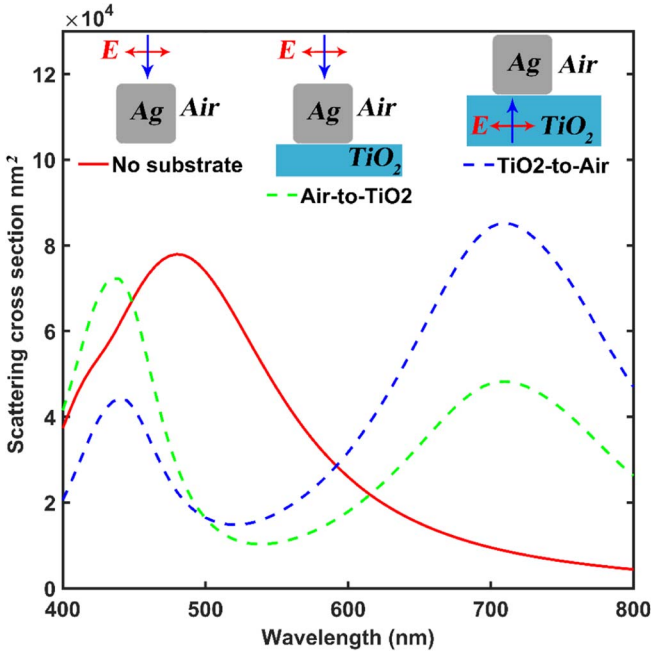

Figure 1. Scattering cross sections (in nm^2) calculated for Ag nanocube with edge length of 100 nm in three setups: without dielectric substrate (solid red line), with TiO_2 substrate and light incident from air to TiO_2 (dashed green line), with TiO_2 substrate and light incident from TiO_2 to air (dashed blue line). Insets illustrate the propagation direction and polarization of light.

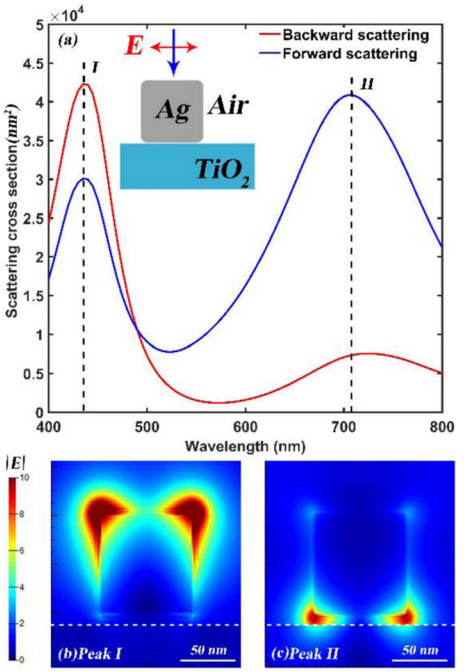

Figure 2. (a) Forward and backward components of scattering cross section of 100-nm Ag nanocube placed on TiO_2 substrate, with the light propagation direction (Air-to-TiO_2) and polarization illustrated by the inset. (b) Near electric field amplitude |E| spatial plot at Peak I (wavelength = 435 nm) as indicated in (a). (c) Near electric field amplitude |E| spatial plot at Peak II (wavelength = 710 nm) as indicated in (a). The white dotted line in (b) and (c) indicates the Air/TiO_2 interface. The plane at which amplitude of electric field is recorded is parallel to paper and is placed 1 nm away from the front face of Ag nanocube.

(Air-to-TiO_2 in short), and the other way around when light is incident from TiO_2 substrate to air (TiO_2-to-Air in short).

In this work, forward scattering cross section refers to the integral of the differential scattering cross section over the forward hemisphere (i.e., integral of all scattered light with scattering angle between 0° to 90°), and backward scattering cross section refers to the integral of the differential scattering cross section over the backward hemisphere (i.e., integral of all scattered light with scattering angle between 90° to 180°).

The Air-to-TiO_2 and TiO_2-to-Air scattering spectrums for Ag nanocube placed on TiO_2 substrate as shown in Fig. 1 are further decomposed into forward and backward scattering, respectively illustrated in Fig. 2a and Fig. 3a. It is observed that the forward scatterings are quite different from the backward scatterings. For the two peaks of the Air-to-TiO_2 scattering as shown in Fig. 1, their near electric field amplitude $|E|$ spatial plots are shown in Figs. 2b and 2c respectively, while for the two peaks of the TiO_2-to-Air scattering, their $|E|$ spatial plots are shown in Figs. 3b and 3c, respectively. In Figs. 2 and 3, by correlating peaks of forward and backward scattering spectrums to respective near field plots, an interesting finding is described in the following. When the end of the nanocube with higher $|E|$, which is the active region of free electrons' resonant oscillation, is nearer to an incident light source (as compared to the other end of the nanocube with lower $|E|$), backward scattering dominates around the peak wavelength; and in the reverse case, i.e., when the end of the nanocube with higher $|E|$ is away from an incident light source, forward scattering dominates around the peak wavelength.

Therefore, from Figs. 2 and 3, for backward scattering, the Air-to-TiO_2 setup may offer a solution for blue light (wavelength of about 440 to 460 nm) selective scattering while the TiO_2-to-Air setup may provide a solution for red light (wavelength of about 620 to 700 nm) selective scattering. In terms of forward scattering, for both setups of Air-to-TiO_2 and TiO_2-to-Air, differences between red light and blue light scattering magnitudes are not significant, so both setups of Air-to-TiO_2 and TiO_2-to-Air may achieve simultaneous selective scattering of blue and red light. Generally, metallic nanoparticle's resonance peak positions as well as magnitude of light scattering are also affected by

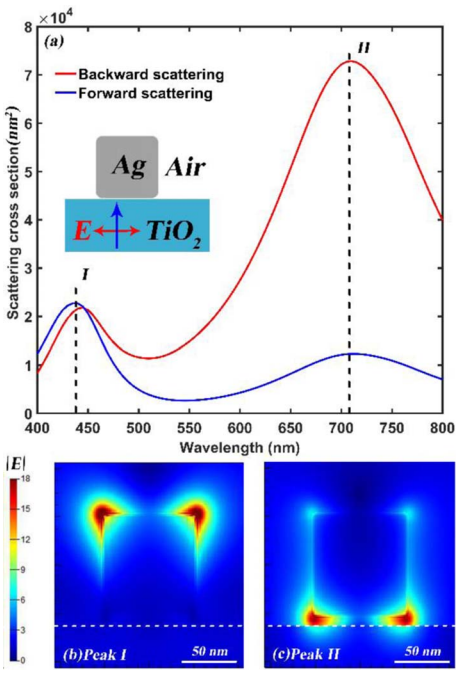

Figure 3. (a) Forward and backward components of scattering cross section of 100-nm Ag nanocube placed on TiO_2 substrate, with light propagation direction (TiO_2-to-Air) and polarization illustrated by the inset. (b) Near electric field amplitude |E| spatial plot at Peak I (wavelength = 440 nm) as indicated in (a). (c) Near electric field amplitude |E| spatial plot at Peak II (wavelength = 710 nm) as indicated in (a). The white dotted line in (b) and (c) indicates the Air/TiO_2 interface. The plane at which amplitude of electric field is recorded is parallel to paper and is placed 1 nm away from the front face of Ag nanocube.

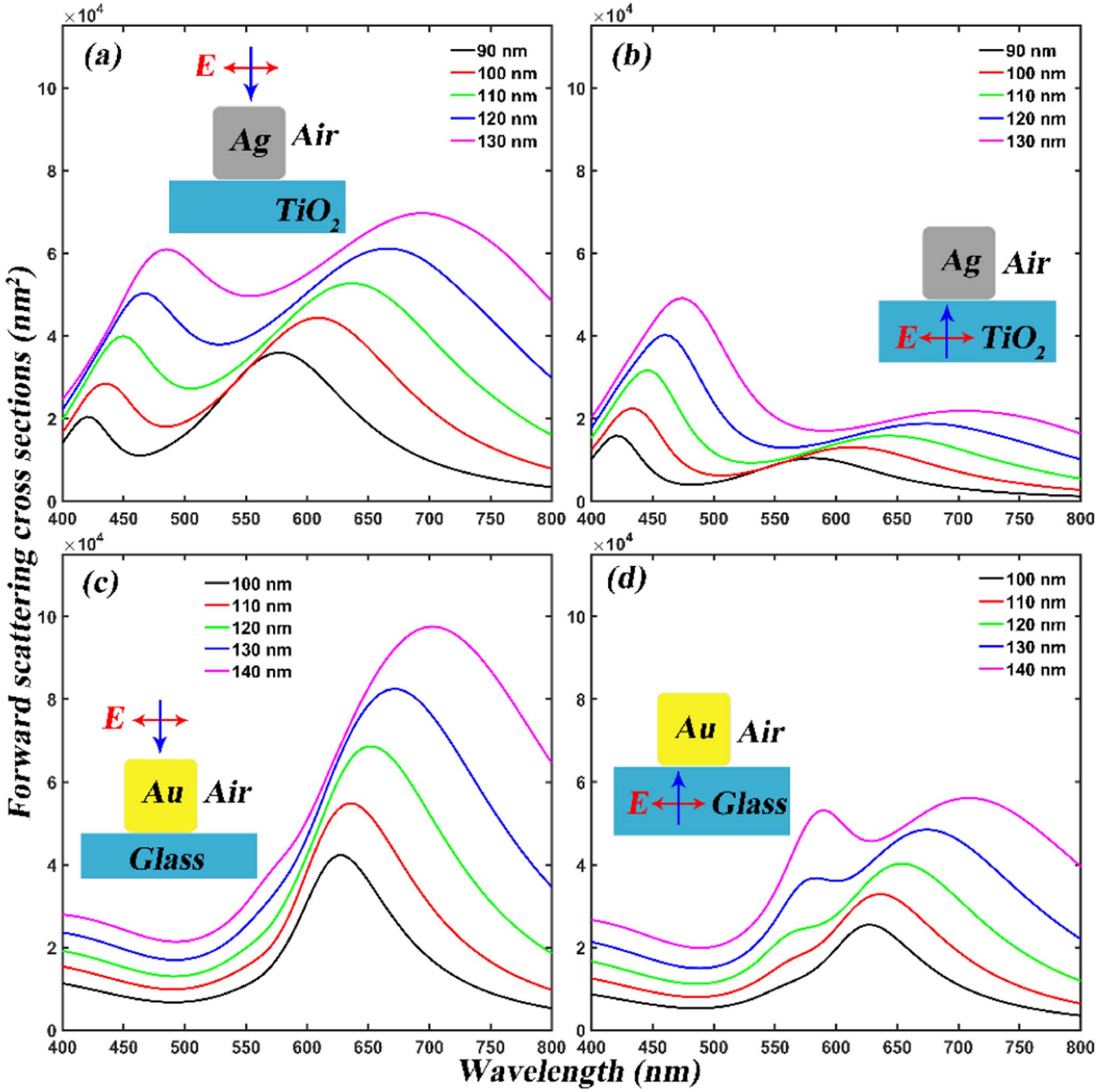

Figure 4. Simulated forward scattering cross sections for TiO_2-substrate/Ag nanocubes are shown in (a) and (b), and for glass-substrate/Au nanocubes are shown in (c) and (d). Incident direction and polarization of light for each sub-figure are illustrated by its corresponding inset. Figure legends denote the edge lengths of nanocubes. For all simulations shown in this figure, a 2-nm gap between the bottom of nanocube and the dielectric substrate is assumed to simulate the protective reagent in a real situation,[2] such as PVP (Polyvinyl Pyrrolidone). The scale of the vertical axis is the same for all sub-figures for easy comparison.

metallic nanoparticle's size.[19,20] With the above considerations, forward (Figs. 4a and 4b) and backward (Figs. 5a and 5b) scattering cross sections are calculated for TiO_2 substrate/Ag nanocubes of several sizes (edge length = 90, 100, 110, 120, and 130 nm), for both setups of Air-to-TiO_2 and TiO_2-to-Air, to search for the best solutions for selective scattering of blue and red light.

From Figs. 4a and 4b and Figs. 5a and 5b, it is observed that the scattering peaks intended for red light selective scattering at longer wavelengths are broader than those intended for blue light selective scattering at shorter wavelengths, but narrow scattering peak width is more desirable. To search for red light scattering peak with narrow width, forward (Figs. 4c and 4d) and backward (Figs. 5c and 5d) scattering cross sections are calculated for glass substrate/Au nanocubes of several sizes (edge length = 100, 110, 120, 130, and 140 nm), for both setups of Air-to-Glass (light is incident from air to glass) and Glass-to-Air (light is incident from glass to air). The reason to investigate scattering properties of Au nanocubes is that Au has a high quality factor (defined by $-Re[\varepsilon]/Im[\varepsilon]$, where ε is metal's dielectric function, and the higher this value, the stronger the resonance strength) around the wavelength range of red light,[21] which suggests Au nanocubes may generate sharp and strong scattering peaks for red light. The reason for choosing glass rather than TiO_2 as the dielectric substrate for Au nanocubes is given as follows. The simulation results obtained with TiO_2-substrate (shown in the supplementary material)

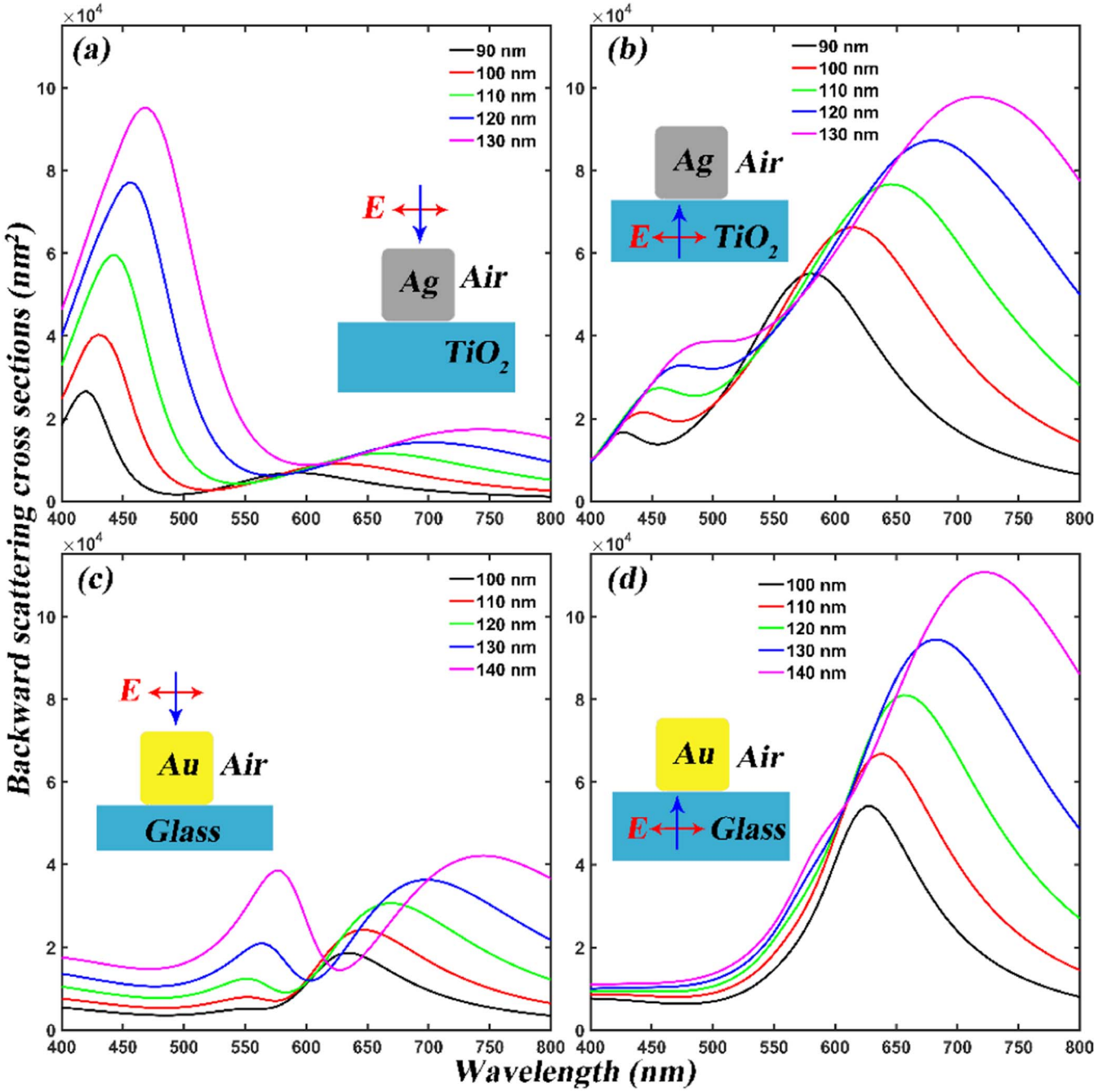

Figure 5. Simulated backward scattering cross sections for TiO_2-substrate/Ag nanocubes are shown in (a) and (b), and for glass-substrate/Au nanocubes are shown in (c) and (d). Incident direction and polarization of light for each sub-figure are illustrated by its corresponding inset. Figure legends denote the edge lengths of nanocubes. For all simulations shown in this figure, a 2-nm gap between the bottom of nanocube and the dielectric substrate is assumed to simulate the protective reagent in a real situation,[2] such as PVP (Polyvinyl Pyrrolidone). The scale of the vertical axis is the same for all sub-figures for easy comparison.

suggest that due to TiO_2's high refractive index, there is a trade-off between resonance peak wavelength and magnitude of scattering, i.e., when increasing Au nanocube's size to increase magnitude of scattering cross section to a desirable value, the resonance peak wavelength is undesirably redshifted beyond 700 nm at the meantime.

A suitable scattering peak for selective scattering of blue or red light should satisfy two criteria: first, the magnitude of scattering cross section around the peak wavelength should be as large as possible, because for transparent projection screen based on the dielectric substrate/metallic nanocubes structure, only one layer of metallic nanocubes can be deposited; second, the peak wavelength should be within the desirable wavelength ranges, i.e., for blue light scattering, the peak wavelength should be within the range of 440–460 nm, and for red light scattering, the peak wavelength should be within 620–700 nm. Therefore, according to these criteria and based on the observations from Figs. 4 and 5, suitable setups for selective scattering of blue and red light can be summarized as:

1. Forward scattering of blue light: 120 nm Ag nanocube with TiO_2-to-Air (Fig. 4b blue curve).

2. Forward scattering of red light: 120 nm Ag nanocube with Air-to-TiO_2 (Fig. 4a blue curve), and 130-nm Au nanocube with Air-to-Glass (Fig. 4c blue curve).
3. Backward scattering of blue light: 120 nm Ag nanocube with Air-to-TiO_2 (Fig. 5a blue curve).
4. Backward scattering of red light: 120 nm Ag nanocube with TiO_2-to-Air (Fig. 5b blue curve), and 130-nm Au nanocube with Glass-to-Air (Fig. 5d blue curve).

Therefore, the following two combinations can achieve forward simultaneous selective scattering of blue and red light: 120 nm Ag nanocube with TiO_2-to-Air (Fig. 4b) blue curve) + 120 nm Ag nanocube with Air-to-TiO_2 (Fig. 4a blue curve), and 120 nm Ag nanocube with TiO_2-to-Air (Fig. 4b blue curve) + 130 nm Au nanocube with Air-to-Glass (Fig. 4c blue curve). Similarly, to achieve backward simultaneous selective scattering of blue and red light, there are also two combinations: 120 nm Ag nanocube with Air-to-TiO_2 (Fig. 5a blue curve) + 120-nm Ag nanocube with TiO_2-to-Air (Fig. 5b blue curve), and 120 nm Ag nanocube with Air-to-TiO_2 (Fig. 5a blue curve) + 130-nm Au nanocube with Glass-to-Air (Fig. 5d blue curve). Note that the combination (120-nm Ag nanocube with Air-to-TiO_2) + (120 nm Ag nanocube with TiO_2-to-Air) appears both in forward and backward scattering, which indicates that this combination can achieve both forward and backward selective scattering of blue and red light. Therefore, there are only three combinations for simultaneous scattering of blue and red light:

1. Forward scattering: (120 nm Ag nanocube with TiO_2-to-Air) + (130 nm Au nanocube with Air-to-Glass)
2. Backward scattering: (120 nm Ag nanocube with Air-to-TiO_2) + (130 nm Au nanocube with Glass-to-Air)
3. Forward and backward scattering: (120 nm Ag nanocube with Air-to-TiO_2) + (120-nm Ag nanocube with TiO_2-to-Air)

The schematics of the three combinations are shown in insets of Fig. 6, with TiO_2 as coating layer(s) on glass, and glass as the substrate. The interface between two different media reflects light, thus the amount of light reaching the back side (as opposed to the side where incident light is injected) of the TiO_2-coated glass slip is reduced, which decreases scattering of metallic nanocubes placed on this side. Therefore, it is important to reduce light reflection by properly selecting thickness of TiO_2 layer(s) coated on glass. For the first combination, it is desirable to reduce reflection of red light because Au nanocube placed on the back side is responsible for red light backward scattering. Reduction of red-light reflection can be achieved by a destructive interference between the light reflected at the air/TiO_2 interface and the light reflected at the TiO_2/glass interface. Light reflection at the air/TiO_2 interface has a phase-shift of 180°, while light reflection at the TiO_2/glass (TiO_2/air) has no phase-shift, so a destructive interference between these two reflections is realized by choosing the TiO_2 thin film's thickness to be $\lambda_{red}/(2n)$, where λ_{red} is the red light's wavelength in vacuum and is chosen to be 650 nm in our work, and n is the refractive index of the TiO_2 thin film which is measured to be 2.3. Thus, thickness of the TiO_2 thin film for the first combination is decided to be 137 nm. Similarly, for the second combination, because Ag nanocube placed on the back side is responsible for blue light forward scattering, reduction of blue light reflection is desired and thickness of the TiO_2 thin film of this combination is decided to be 100 nm. For the third combination, Ag nanocube placed on the back side is responsible for both blue and red light scattering, so to achieve a balance, the wavelength at which the light's reflection to be minimized is selected to be 550 nm, leading to a thickness of 120 nm for TiO_2 thin film of this combination.

For the first combination, backward scattering from Ag nanocube is combined with that from Au nanocube, with consideration of TiO_2 thin film's thickness and light reflections at all interfaces, and is shown as an overall backward scattering in Fig. 6a. Similarly, combined overall forward scattering for the second combination is shown in Fig. 6b, and both combined overall forward and backward scattering spectrums for the third combination are shown in Fig. 6c.

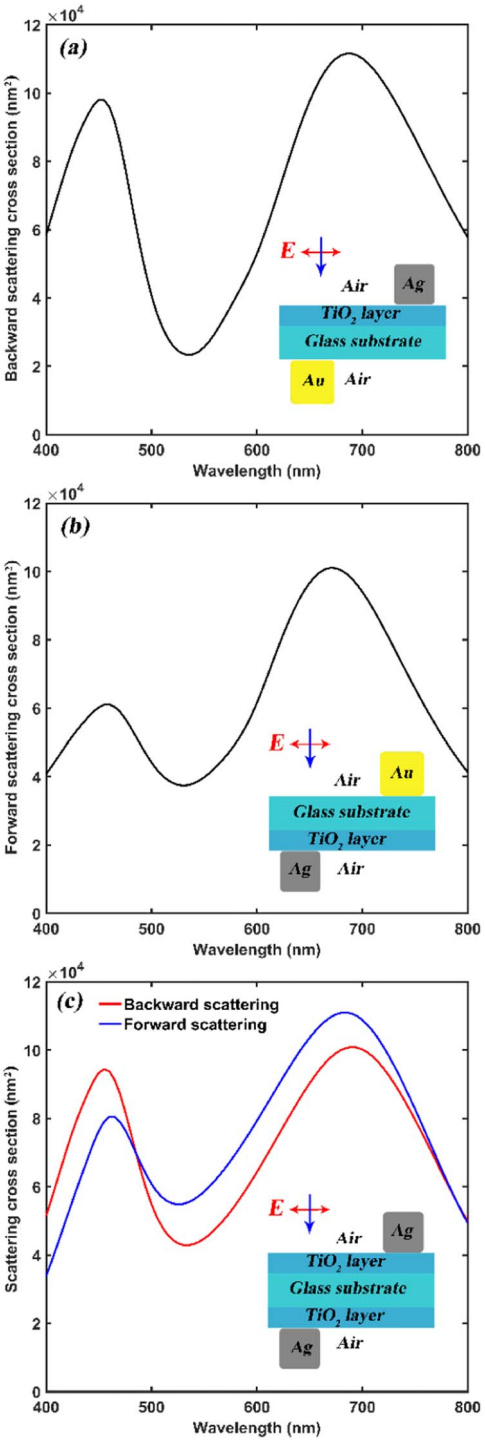

Figure 6. Combined overall forward or backward scattering cross sections for the three combinations discussed in text, with their schematics shown by insets, and effect of TiO_2 thin film's thickness and light reflections at all interfaces are considered for all three combinations. (a) Overall backward scattering for the first combination combined from that of Ag nanocube and Au nanocube, thickness of the TiO_2 thin film is 137 nm. (b) Overall forward scattering for the second combination combined from that of Ag nanocube and Au nanocube, thickness of the TiO_2 thin film is 100 nm. (c) Overall forward scattering as well as backward scattering for the third combination combined from that of Ag nanocube at the foreside and that of Ag nanocube at the back side, thickness of both the two TiO_2 thin films is 120 nm. In (a), (b) and (c), Ag nanocube's edge length is 120 nm. In (a) and (b), Au nanocube's edge length is 130 nm. For all simulations shown in this figure, a 2-nm gap between the bottom of nanocube and the dielectric substrate is assumed to simulate protective reagent in a real situation,[2] such as PVP (Polyvinyl Pyrrolidone).

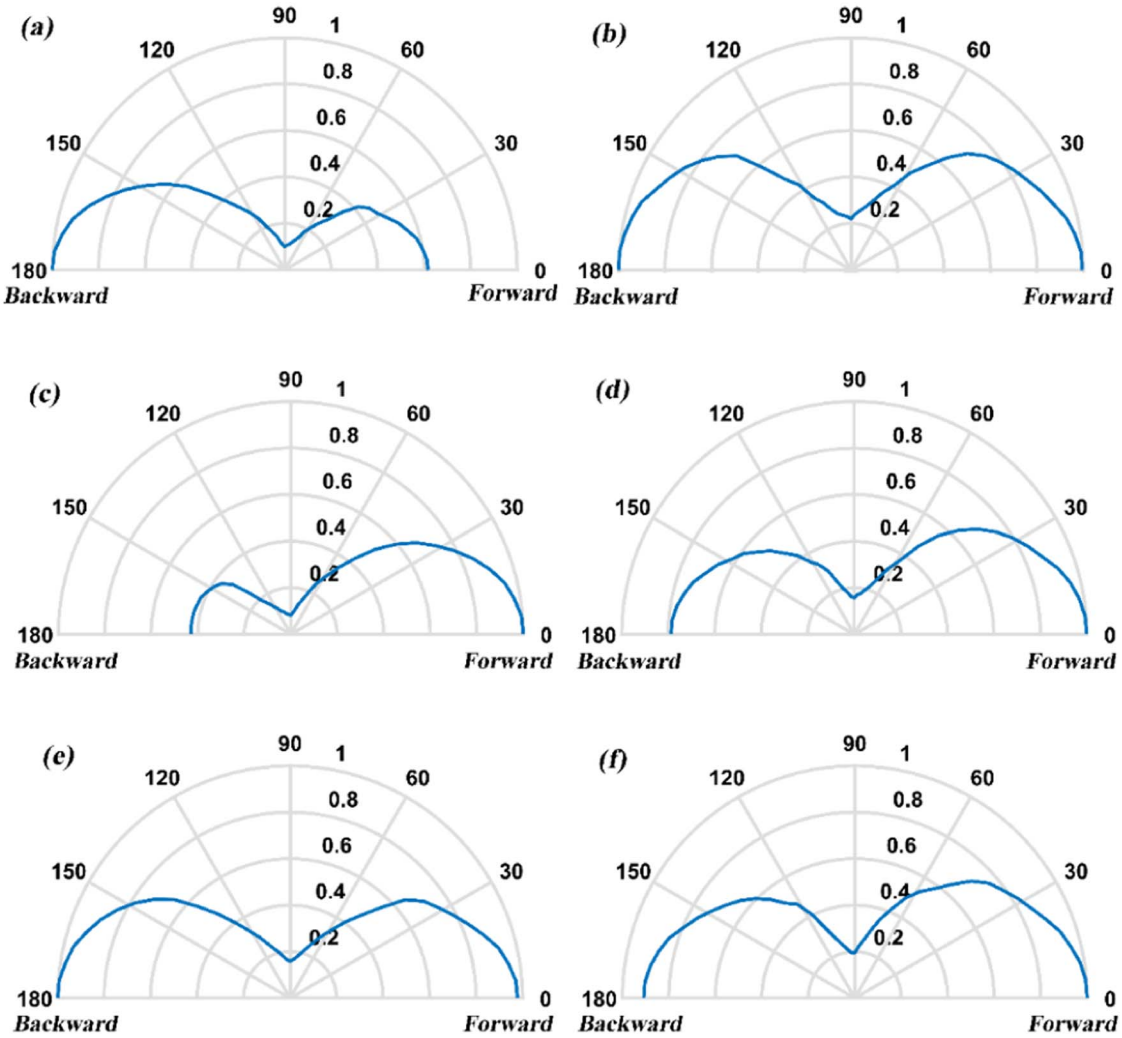

Figure 7. Normalized scattering intensity $|E|^2$ plotted versus scattering angle for the three combinations shown in Figure 6. (a) Plotting for the first combination at the wavelength of 455 nm. (b) Plotting for the first combination at the wavelength of 680 nm. (c) Plotting for the second combination at the wavelength of 460 nm. (d) Plotting for the second combination at the wavelength of 680 nm. (e) Plotting for the third combination at the wavelength of 460 nm. (f) Plotting for the third combination at the wavelength of 685 nm. All scattering intensities shown in this figure consist of contributions from both the nanocubes placed on the foreside and back side of the TiO_2-coated glass slide. Incident light has equal components for s- and p- polarisations with respect to the scattering plane. Each sub-figure's angular distribution of scattering intensity is normalized to its largest value.

From Fig. 6, it is observed that all three combinations achieve selective enhancement of blue and red light scattering, either in forward or backward or both directions. And given a scattering cross section of about 50000 nm^2 at peak wavelength for a single nanoparticle is able to generate a clear projected image with proper areal nanoparticle density as demonstrated in previous work,[2] all three combinations as shown in Fig. 6 have enough magnitudes of scattering and are expected to generate clear projected image with suitable areal concentration of nanocubes. In Fig. 6b, the relative weaker peak around 455 nm for blue light forward scattering can be strengthened by increasing areal concentration of Ag nanocubes deposited on the back side of the TiO_2-coated glass slide relative to that of Au nanocubes deposited on the foreside in a real application. For each combination shown in Fig. 6, angular distribution of scattering is plotted for both peaks and shown in Fig. 7.

From Fig. 7, it is observed that the angular distribution of scattering is relatively isotropic for both peaks in backward direction (90° to 180°) for the first combination, in forward direction (0° to 90°) for the second combination, and in both forward and backward directions (0° to 180°) for the third combination. These indicate projected image can be viewed clearly within a reasonable angle range (refer to the polar plots in Fig. 7 for angles stated here): about 135° to 180° for the combinations suitable for backward scattering (combinations 1 and 3), and about 0° to 50° for the combinations suitable for forward scattering (combinations 2 and 3).

Conclusions

In this work, through numerical simulations, forward and backward scattering properties of Ag and Au nanocubes placed on dielectric substrate are investigated, with effect of nanocube's size and both setups of Air-to-Dielectric (light is incident from air to dielectric) and Dielectric-to-Air (light is incident from dielectric to air) taken into account. Based on the forward and backward scattering properties, three designs (the three combinations shown in Fig. 6) are proposed, two of which achieve selective scattering of blue and red light only in either forward or backward direction, and the other one achieves selective scattering of blue and red light both in forward and backward directions, all with reasonable large magnitudes of scattering strength.

Simulated angular distribution of scattering suggests that the viewing-angle range is large for all the three designs.

Acknowledgment

This work was financially supported by the National Research Foundation of Singapore (Program grant No. NRF-CRP13-2014-02).

ORCID

Yiyang Ye https://orcid.org/0000-0003-0215-8736

References

1. C. W. Hsu, B. Zhen, W. Qiu, O. Shapira, B. G. DeLacy, J. D. Joannopoulos, and M. Soljačić, *Nat. Commun.*, **5**, 3152 (2014).
2. K. Saito and T. Tatsuma, *Nanoscale*, **7**(48), 20365 (2015).
3. A. Monti, A. Toscano, and F. Bilotti, *Journal of Applied Physics*, **121**(24), 243106 (2017).
4. Y. Ye, T. Chen, J. Zhen, C. Xu, J. Zhang, and H. Li, *Nanoscale*, **10**(5), 2438 (2018).
5. J. Schanda, in *Encyclopedia of Color Science and Technology*, R. and Luo, ed., p. 1, Springer Berlin Heidelberg, Berlin, Heidelberg, (2014).
6. Y. Kane, *IEEE Transactions on Antennas and Propagation*, **14**(3), 302 (1966).
7. D. Mergel, D. Buschendorf, S. Eggert, R. Grammes, and B. Samset, *Thin Solid Films*, **371**(1), 218 (2000).
8. M. Zhang, G. Lin, C. Dong, and L. Wen, *Surface and Coatings Technology*, **201**(16), 7252 (2007).
9. H. Fujiwara, *Spectroscopic ellipsometry: principles and applications*, John Wiley & Sons (2007).
10. A. Taflove and S. C. Hagness, *Computational Electrodynamics: The Finite-difference Time-Domain Method*, Artech House, Boston (2000).
11. E. D. Palik, *Handbook of optical constants of solids*, Academic press (1998).
12. U. Kreibig, *Journal of Physics F: Metal Physics*, **4**(7), 999 (1974).
13. S. Zhang, K. Bao, N. J. Halas, H. Xu, and P. Nordlander, *Nano Letters*, **11**(4), 1657 (2011).
14. L. J. Sherry, S.-H. Chang, G. C. Schatz, R. P. Van Duyne, B. J. Wiley, and Y. Xia, *Nano Letters*, **5**(10), 2034 (2005).
15. A. Bottomley and A. Ianoul, *The Journal of Physical Chemistry C*, **118**(47), 27509 (2014).
16. M. W. Knight, Y. Wu, J. B. Lassiter, P. Nordlander, and N. J. Halas, *Nano Letters*, **9**(5), 2188 (2009).
17. Y. Wu and P. Nordlander, *The Journal of Physical Chemistry C*, **114**(16), 7302 (2010).
18. K. C. Vernon, A. M. Funston, C. Novo, D. E. Gómez, P. Mulvaney, and T. J. Davis, *Nano Letters*, **10**(6), 2080 (2010).
19. K. L. Kelly, E. Coronado, L. L. Zhao, and G. C. Schatz, *J. Phys. Chem. B*, **107**(3), 668 (2003).
20. U. Kreibig and M. Vollmer, *Optical properties of metal clusters*, Springer Science & Business Media (2013).
21. M. G. Blaber, M. D. Arnold, and M. J. Ford, *The Journal of Physical Chemistry C*, **113**(8), 3041 (2009).